A new approach for modeling the Cenozoic oceanic lithium isotope paleo-variations : the key role of climate

Nathalie Vigier[1] & Yves Godderis[2]

[1]Laboratoire d'Océanographie de Villefranche, CNRS, UPMC, 06230 Villefranche sur Mer, France. nathalie.vigier@obs-vlfr.fr (for correspondance)

[2]Géosciences Environnement Toulouse, CNRS, Université Paul Sabatier, 31400 Toulouse, France

Abstract

The marine record of the ocean lithium isotope composition may provide important information constraining the factors that control continental weathering and how they have varied in the past. However, the equations establishing the links between the continental flux of Li to the ocean, its Li isotope composition and the ocean Li isotope composition are under-constrained, and their resolution are related to significant uncertainties. In order to partially reduce this uncertainty, we propose a new approach that couples the C and Li cycles, such that our proposed reconstruction of the Cenozoic Li cycle is compatible with the required stability of the exospheric carbon cycle on geological timescales. The results of this exercise show, contrary to expectations, that the Cenozoic evolution of the Li isotope composition of rivers does not have necessarily mimicked the oceanic δ^7Li rise. In contrast, variations in the continental flux of Li to the ocean are demonstrated to play a major role in setting the ocean δ^7Li. We also provide evidence that Li storage in secondary phases is an important element of the global Li cycle that cannot be neglected, in particular during the early Cenozoic. Our modeling of the published foraminifera record highlight a close link between soil formation rate and indexes recording the climate evolution during the Cenozoic, such as foraminifera δ^{18}O and pCO_2 reconstructions. This leads us to conclude that Li isotope record does not provide a persuasive, unique evidence for an erosional forcing of Cenozoic change, because it could alternatively be consistent with a climate control on soil production rates.

1. **Introduction**

Weathering (chemical erosion) of continental Ca-Mg rich silicates serves as a major sink of atmospheric CO_2. However, determining how such weathering has evolved in the past, as a function of climate or tectonic activity, remains a challenge. Filling this gap in our knowledge is essential if we are to understand how global temperature is regulated on geological timescales. The great potential of lithium isotopes to trace alteration processes has recently been highlighted (see e.g. review in Burton & Vigier, 2011). Nevertheless, analytical difficulties have limited their use as a marine paleoproxy. Misra & Froelich (2012, 2014) determined the evolution of the lithium isotopic composition of bulk carbonates and planktonic foraminifera over the past 68 Ma. These authors argue that this record reflects ocean-wide variations, and that the 9‰ increase of the marine δ^7Li from the Paleocene to the present (see figure 1), can be explained by an increase of river δ^7Li from 3‰ 60 Ma ago, to 23‰ at present. To account for such a rise in riverine δ^7Li Misra and Froelich (2012) invoke a change of the alteration regime (from a congruent to a weathering- limited regime) and an increase of clay formation (which fractionates Li isotopes) in mountainous - rapidly eroding - areas. This assertion links the secular increase in the marine δ^7Li record to increasing tectonic uplift and mountain building over the course of the Cenozoic. Under this interpretive framework, continental weathering during the early Paleogene (≈ 60 Myrs ago) was characterized principally by high dissolution rates of continental rocks and relatively low rates of clay formation and transport. Such a weathering regime offers a mechanism for producing low δ^7Li values in rivers, close to that of the continental crust, because dissolution is not accompanied by significant Li isotope fractionation. Later in the Cenozoic, as tectonic activity intensifies, incongruent weathering and clay formation is supposed to become more significant, leading to a shift to larger riverine δ^7Li.

However, several lines of evidence call this interpretation of the seawater record into question, and in particular the notion that low δ^7Li values in rivers of the Cretaceous could be sustained by predominately congruent weathering (Wanner et al., 2014). Indeed, a congruency of the weathering process, that would correspond to small rates of clay formation or soil production, at 60 Ma is not supported by the occurrence of thick weathering profiles found at this period of time (e.g. Beauvais & Chardon, 2013; Tavlan et al., 2011; Meshram & Randiv, 2011). In particular, the compilation of laterite formation by Beauvais and Chardon (2013) shows that a major episode of laterite formation is centered on 55 Ma in West Africa,

87 at the time of the climatic optimum (Zachos et al., 2008) and when West Africa was located
88 in the warm and humid convergence zone. Laterite profiles have also been identified at high
89 latitudes during the same time interval. At least four spikes of lateritic formation are recorded
90 between 55 and 48 Man the cause of it being identified as global warming (e.g. Retallack,
91 2010; 2014). A compilation of about 80 ODP or DSDP core sites indicate that the deep
92 seawater during the Paleocene exhibited low $\delta^{18}O$ values, with benthic foraminifera $\delta^{18}O$
93 values between 3 and 4 ‰ lower than at present (Zachos et al., 2001). This feature is
94 interpreted as much warmer climatic conditions, in agreement with recent reconstructions of
95 atmospheric pCO_2 at 60 Ma, ranging between 400 and 1000 ppmv (Beerling & Royer, 2011).
96 These conditions have favored the formation of thick weathering profiles, in particular of
97 lateritic regolith mantles rich in kaolinite and/or bauxite. These resistant phases are depleted
98 in major cations playing a key role in the carbon cycle (such as Ca and Mg), but they contain
99 significant amounts of Li. Our compilation of Li levels in kaolinite-rich samples (Table 1)
100 shows that they are - on average - similar to the Li content estimated for the continental crust
101 granites (22ppm±4ppm, Teng et al., 2009). They may therefore have played a key role in the
102 continental Li cycle. Li-containing regoliths provide empirical evidence against the idea that
103 congruent weathering prevails during warm intervals of Earth history driving riverine $\delta^{7}Li$ to
104 values similar to average upper crust.
105 In this study, we propose a new modeling approach of the seawater record that consists in
106 coupling a simple mathematical description of the carbon and the lithium exospheric budget,
107 throughout the Cenozoic. The objective is not to produce an exhaustive study of the impact of
108 each parameter implied in the Li and the C cycle, but rather to show that for a given set of
109 parameters consistent with published estimations, there is an alternative solution that can
110 explain the Cenozoic $\delta^{7}Li$ oceanic variations.
111 Our model takes into account the changes in Li flux coming from the continents in response
112 to a balance between 1/ dissolution rates of continental rocks releasing Li in waters and 2/
113 temporary storage of Li into secondary phases formed in weathering profiles. Since lithium
114 isotopes fractionate during clay mineral accumulation (e.g. Huh et al., 2001; Kisakurek et al.,
115 2004; Rudnick et al., 2004), soil formation rate is expected to drive the Li isotope
116 composition of rivers. One illustration is that, at present, the mean $\delta^{7}Li$ value of the
117 continental runoff (+23‰; Huh et al., 1998) is much higher than the average $\delta^{7}Li$ value
118 estimated for the continental crust granites (+2±4‰, Teng et al, 2009). Since Li isotopes do
119 not fractionate during dissolution, this difference is best explained by isotope fractionation

during the formation of secondary phases (Vigier et al., 2009; von Strandmann et al., 2010; Bouchez et al., 2013). Consequently, at present, at the world-wide scale, a significant part of the Li released by continental dissolution is stored in ^{6}Li-rich soils, resulting in heavy signatures (^{7}Li-rich) in rivers. Experimental investigations, as well as soil studies support these findings (e.g. Wimpenny et al., 2010; Vigier et al., 2008; Lemarchand et al, 2010). Thus, we explore how Li storage in soils at the global scale has affected the ocean δ^{7}Li value, as well as the potential of ocean δ^{7}Li to quantify the balance between physical denudation and chemical alteration and its variation throughout the Cenozoic.

2. Model equations and basics

2.1. Seawater isotopic balance

The two main sources of dissolved lithium to the ocean (oc) are river waters (riv) and high temperature hydrothermal fluids (hyd) (see Huh et al., 1998 and a detailed review in Tomascak, 2004 and in the supplementary material of Misra and Froelich, 2012). The main sink of oceanic lithium is its incorporation into authigenic phases, in particular marine clays which are the marine phases the most enriched in Li (Chan et al. , 2006). The seawater isotopic mass balance can thus be written as :

$$M^{Li}_{oc}.d\delta_{oc}/dt = F_{riv}(\delta_{riv}-\delta_{oc})+F_{hyd}(\delta_{hyd}-\delta_{oc})-F_{clay}(\delta_{oc}-\Delta_{oc}-\delta_{oc}) \quad (1)$$

where F is for the Li flux, and δ_{riv} δ_{oc} and δ_{hyd} are for the δ^{7}Li values of rivers, ocean and hydrothermal fluids respectively. Δ_{oc} represents the absolute value of the fractionation factor of the Li isotopes during marine secondary phase formation. In the literature, this factor is negative (preferential enrichment of the light ^{6}Li isotope) and ranges between -10 and -25‰ depending on the temperature at which authigenic phases are being formed (Chan et al, 1992; 1993; Vigier et al., 2008).

The residence time of Li in the ocean is equal to 1 million years. Given that we are exploring the time evolution of its isotopic cycle over the whole Cenozoic (10^{7} year timescale), we can assume steady-state for both the elemental (i.e. all the Li carried by rivers and released by hydrothermal activity into the ocean is removed through authigenic clay formation: $F_{riv} + F_{hyd}$

153 = F_{clay}) and isotopic Li cycles. The steady-state hypothesis is only valid for a timescale of
154 several million years (at least three times the Li residence time in the ocean).
155
156 Equation (1) becomes:
157 $$F_{riv}(\delta_{riv}-\delta_{oc})+F_{hyd}(\delta_{hyd}-\delta_{oc})+F_{riv}.\ \Delta_{oc}+F_{hyd}.\ \Delta_{oc}=0 \quad (2)$$
158
159 Consequently, we can solve the above equations for δ_{oc}:
160 $$\delta_{oc}=(F_{riv}\delta_{riv}+F_{hyd}\delta_{hyd}+\Delta_{oc}.(F_{riv}+F_{hyd}))\ /\ (F_{riv}+F_{hyd}) \quad (3)$$
161
162 where present-day published values for F_{riv}, F_{hyd} and Δ_{oc} are reported in Table 2. We consider
163 that the hydrothermal flux during the Cenozoic decreased slightly as a function of time,
164 following the curve described in Engebretson et al. (1992), based on variations of subduction
165 rates and mid-ocean ridge volume. This trend is currently used in numerical modeling of the
166 global carbon cycle and appears to be consistent with the Cenozoic climatic evolution
167 (Berner, 2004; Lefebvre et al., 2013).
168
169 Basically, equation 3 has two unknowns: F^{Li}_{riv} and δ_{riv}. In previous studies (Hathorne and
170 James, 2006; Misra & Froelich, 2012), river δ^7Li has been interpreted as co-varying in a
171 straightforward way with the ocean δ^7Li. However, one equation is not enough for two
172 independent unknowns. In contrast to the a priori expectation, the variation of the ocean δ^7Li
173 composition during the Cenozoic may not reflect riverine δ^7Li variations in a straightforward
174 way. The reason for this is that it strongly depends on the continental Li flux too, which is
175 likely to have been strongly affected by variation in continental weathering rates during this
176 period of time. One purely theoretical example of the influence of the Li continental flux is
177 illustrated in Figure 2. This simulation shows that the 0-65Ma foraminifera δ^7Li record
178 (shown in figure 1) can still be fitted by imposing a constant river δ^7Li throughout the
179 Cenozoic, and using parameters values which are consistent with published data (Table 2).
180 We fixed the δriv (δ^7Li in rivers) to its present-day value (23‰). This is an extreme and
181 unlikely scenario because it does not account for change in the isotope fractionation due to
182 continental weathering. Indeed, the riverine δ^7Li is expected to vary as a function of the
183 relative importance of dissolution rate and clay formation rate (e.g. Bouchez et al., 2013).
184 However, this simulation shows that, by taking into account the Li ocean budget only, the
185 system of equations is under-constrained and it is not possible to calculate the temporal

variations of riverine δ^7Li without making assumptions about the link between F^{Li}_{riv} and δ_{riv}. It also shows that low seawater δ^7Li, as highlighted by early Eocene foraminifera can be compatible with a high δ^7Li value of the riverine flux. Our result shows therefore that low δ^7Li in the ocean does not systematically imply low river δ^7Li. The temporal variations of the riverine Li flux also need to be established. In the following, we add constraints on this aspect and the Li cycle, by coupling it to the carbon cycle.

2.2. Walker paleothermostat

The Walker paleothermostat (Walker et al., 1981) implies that, at the million year scale, the consumption of carbon by silicate weathering (F_{riv}^{CO2}) closely balances the release by volcanic degassing (assumed to be proportional at first order to the seafloor spreading rate, and hence to the hydrothermal activity) (F_{hyd}^{CO2}), a condition absolutely needed to avoid unrealistic atmospheric CO_2 fluctuations (Godderis & François, 1995; Kump & Arthur, 1997):

$$F_{hyd}^{CO2} = F_{riv}^{CO2} \quad (4)$$

During high temperature water-rock interactions, Li is known to be highly mobile, as reflected by the large Li concentrations found in hydrothermal fluids located in mid-ocean ridges (ppm level, Chan et al., 1994; Foustoukos et al., 2004; Mottl et al., 2011), and which are ~3 orders of magnitudes greater than in river waters or seawater. Consequently, we consider that the amounts of Li released by hydrothermal process is proportional to the carbon flux released into the ocean:

$$F_{hyd}^{CO2} = k_2 F_{hyd}^{Li} \quad (5)$$

with k_2 = (C/Li) of hydrothermal fluids (Table 2)

In contrast with hydrothermal conditions, Li is much less "mobile" on the continents, as reflected by low Li contents in river waters (ppb level) while granites (the main source of river Li) are enriched in Li compared to oceanic crust. Indeed, first, thermodynamic laws indicate that dissolution rate is lower at lower temperature. Additionally, it is observed that most of the Li carried by rivers to the ocean is mainly located in the particulate load (>70%, e.g. Millot et al., 2010), while the dissolved Li represents only a minor proportion. This is

consistent with the fact that Li can be significantly incorporated into the structure of secondary minerals, mainly clays. As a consequence, the flux of dissolved Li carried by rivers may not be proportional to the flux of CO_2 consumed during the leaching or dissolution of continental mineral phases. The relationship linking the flux of lithium carried by rivers and the flux of atmospheric CO_2 consumed by mineral dissolution becomes:

$$F_{riv}^{CO2} = 1/k_1 . F^{Li}_{diss} = (F^{Li}_{riv} + F^{Li}_{sp}) / k_1 \quad (6)$$

F^{Li}_{riv} and F^{Li}_{sp} being the flux of lithium in river waters and in secondary phases respectively, and F^{Li}_{diss} the flux of Li released into continental waters during the dissolution of continental rocks ($F^{Li}_{riv} = F^{Li}_{diss} - F^{Li}_{sp}$). k_1 is calculated assuming that dissolution of continental rocks release Li, Mg and Ca congruently. Also, we consider that 1 mol of atmospheric CO_2 is consumed by the dissolution of 1 mol of Mg+Ca present in continental rocks (accounting for the subsequent carbonate precipitation in the ocean) (Berner, 2004). Consequently, $k_1 = Li_{UCC} / (Ca + Mg)_{UCC}$ (UCC being the Upper Continental Crust, Table 2).

If present-day conditions might reflect a recent disequilibrium due to the last glaciation (Vance et al., 2009), at the Cenozoic timescale, formation of thick weathering profiles with significant residence time (>0.5Ma) are likely to have impacted the Li cycle. We assume that most of secondary phases present in these profiles are largely depleted in cations, in particular in Ca and Mg, and therefore do not affect significantly the carbon budget. This is a first order approximation. Indeed, laterite in which the largely dominant clay phase is Mg-Ca free kaolinite, covers only 30% of the continental surfaces. However, owing to their thickness, they constitute about 85% of the global continental pedogenic cover (Nahon, 2003), supporting the above assumption.

Combining equation (4) (5) and (6) we obtain the following relationship:

$$F^{Li}_{riv} = k_1 . k_2 F_{hyd}^{Li} - F^{Li}_{sp} \quad (7)$$

where the flux of riverine Li is a function of both the hydrothermal flux and of the secondary phase formation rate on the continents.

2.3. Riverine $\delta^7 Li$

All published studies indicate the existence of a strong isotope fractionation during the formation of secondary phases, such as clays or Fe oxides, always in favor of the light isotope (^{6}Li). At periods when the soil production increased in the past due to increase rate of secondary phase formation, we therefore expect that the δ^7Li of river waters increase, since more ^{6}Li is incorporated and stored into soils. In fact, the riverine δ^7Li is the result of the competition (e.g. Bouchez et al., 2013, Vigier et al., 2009) between the isotopically congruent dissolution of fresh bedrock, and the precipitation of secondary phases with an isotope fractionation Δ_{land} (Table 2), such that:

$$F^{Li}_{riv}\delta_{riv} = \delta_{UCC}.F^{Li}_{diss}-F^{Li}_{sp}.(\delta_{riv}- \Delta_{land}) \quad (8)$$

with δ_{UCC} being the average δ^7Li value estimated for the upper continental crust (Table 2). Given that $F^{Li}_{diss} = F^{Li}_{riv} + F^{Li}_{sp}$, equation (8) becomes:

$$\delta_{riv}= \delta_{UCC} + (F^{Li}_{sp}\ \Delta_{land}) / (F^{Li}_{riv} + F^{Li}_{sp}) \quad (9)$$

This equation states that , if $F^{Li}_{sp} = 0$, then δ_{riv} equals $\delta_{UCC.}$ Otherwise, δ_{riv} is higher than δ_{UCC}. To date the published values of δ^7Li of most rivers (e.g. Huh et al., 1998, Millot et al., 2010; Kisakurek et al., 2004) are significantly greater than the δ^7Li estimated for UCC (2‰ , Teng et al. 2009), and thus are consistent with equation (9).

2.4. Method for solving the model

We assume that the foraminifera δ^7Li reflect the ocean δ^7Li, as assumed in Misra & Froelich (2012) and in Hathorne & James (2006). We consider that potential vital effects, responsible for changes of Li isotope fractionation during foraminifera growth may explain some observed rapid (<0.5Ma) changes of foraminifera Li isotope compositions, but we do not take into account these effects since the model aims at working at the multi million scale only. A moving average of the oceanic lithium isotopic data is calculated, with a window width of 5 millions of years, since the isotopic steady-state is valid for a timescale of at least three times the Li residence time in the ocean (see figure 1). This data smoothing therefore ensures the validity of the steady-state hypothesis and removes all short term fluctuations potentially related to vital effects.

The equations describing the seawater isotopic budget (eq. 3), the paleothermostat (eq. 7), and the riverine isotopic budget (eq. 9) define a system of equations where the unknowns are the riverine Li flux as a function of time (F^{Li}_{riv}), the storage flux of Li in soils (F^{Li}_{sp}), and the riverine δ^7Li (δ_{riv}). It can be reduced to the following quadratic equation :

$$A_1 (F^{Li}_{riv})^2 + (\delta_{oc} - \Delta_{oc} - \delta_{UCC} - \Delta_{land}) F^{Li}_{riv} - A_2 = 0. \quad (10)$$

Where A_1 and A_2 are equal to :

$$A_1 = \Delta_{land} / (k_1 k_2 F^{Li}_{Hyd}) \quad (11)$$

$$A_2 = F^{Li}_{Hyd} (\delta_{hyd} - \delta_{oc} + \Delta_{oc}) \quad (12)$$

The values for the various parameters used in the model are described in Table 2. As long as the discriminant of eq. 10 is strictly positive, eq. 10 has two solutions for F^{Li}_{riv}. This means that two radically different histories of F^{Li}_{riv} can both explain the rise of the Li isotopic composition of seawater.

2.5. Comparison with other modeling methods

Recently, two modelings of the Cenozoic δ^7Li variations, different from Misra and Froelich (2012, 2014) (section 1) have been proposed. Wanner et al. (2014) focused on a reactive transport model in order to simulate the Li isotopic composition and content of continental waters. Weathering reactions by sub-surface waters are simulated, considering a prescribed thick regolith which already contains altered material (kaolinite and goethite), above a fresh granite. Kinetic reactions based on transition state theory are used for calculating both the dissolution and precipitation of mineral phases. River water chemistry is then considered to be a simple dilution of these sub-surface waters having reacted with previously formed profiles. Overall, the Wanner et al. (2014) model is designed to simulate finely the time evolution of an already existing regolith profile and its impact on the riverine Li content and isotopic composition. As acknowledged by the authors, the fit of the Cenozoic oceanic δ^7Li curve cannot be computed as it would require the accurate knowledge of the Cenozoic climate and runoff variations, to calculate the Li flux to the ocean as well as its isotopic composition.

317 The Wanner et al. (2014) model is a process-based model, but at this stage, it cannot account
318 for global budget.
319
320 Li and West (2014) proposed 12 different simulations for fitting the Cenozoic ocean δ^7Li,
321 focusing their effort on potential variations of the oceanic Li sink and how this could have
322 affected the ocean δ^7Li. They consider that the two major sinks of ocean Li are marine
323 authigenic alumino-silicate clays (during reverse weathering, at low temperature), and
324 removal into oceanic crust during its alteration by circulating fluids of moderate to high
325 temperatures. Both sinks are considered to be associated with a constant isotope fractionation
326 factor throughout the Cenozoic, but a varying proportion of both is considered to influence
327 the Li and δ^7Li removal flux. Then, a steady-state equation is applied to the ocean, identical to
328 the one used here, and different scenarii are tested to explore the impact of the mathematical
329 formulation of the oceanic Li sinks. Changes of river Li flux are assumed to be dependent on
330 the chemical weathering fluxes calculated by another model (Li and Elderfield, 2013), or
331 following the isotope balance method developed by Bouchez et al. (2013). Hydrothermal Li is
332 estimated from the reconstruction of spreading rate (Muller et al., 2008; Rowley, 2002). No
333 direct coupling with the carbon cycle is made.
334
335 At this stage, it is important to underline that, by coupling Li and C budgets, the solving of
336 our model equations does not require additional or independent assumptions for the
337 continental fluxes (dissolved and particulate) during the Cenozoic. Furthermore, our model is
338 based on budget equations only (for Li and C), and does not include any assumption on the
339 dependence of the fluxes on environmental conditions. The solid Earth degassing is extracted
340 from Egenbretson (1992). Although more recent reconstructions have been published, it has
341 been shown recently that the Engebretson's curve is in good agreement with the Cenozoic
342 climate history (itself reconstructed using a coupled 3D climate-carbon model, see Lefebvre
343 et al., 2013). The precise Cenozoic history of the solid Earth degassing weakly influences our
344 results.
345
346
347
348
349
350

3. Results and discussion

3.1 Paleo-variations of continental weathering

Two solutions have thus been found for the Cenozoic (represented in figure 3A and 3B). The first solution (figure 3A) implies an increase of the riverine δ^7Li over the Cenozoic, associated to a decrease of riverine Li flux with time. This first solution is close to the scenario described in details by Misra & Froelich (2012), arguing for an increasing contribution of orogenesis on silicate dissolution, clay formation and CO_2 consumption towards recent time. In this scenario, sequestration of lithium in clays increased from the past towards the present day.

Our model results demonstrate that a second scenario can also explain the Cenozoic Li isotope record and we will focus on this one in the following because the first one was already investigated in details by Misra & Froelich (2012) and by Li & West (2014). Figure 3B shows that the δ^7Li paleorecord can be due to an increase of the riverine Li flux through the Cenozoic. As illustrated in figure 4, this increase is not due to an increase in the dissolution rate of the silicate lithologies, but is mostly due to the decrease of Li storage in secondary phases. Most Li-rich secondary phase are considered to be formed within soil and lateritic profiles, and even if some have the time to be formed during the river transport, this fraction is likely minor compared to the formation of thick soils and kaolinite-rich laterite. Therefore, we consider that most of the Li storage during silicate alteration occur in soils.

In order to test the robustness of our result, we performed two different simulations, using 1/ the whole set of equations (for both C and Li, see section 2), and 2/ an imposed variation of δ_{riv} that is arbitrarily forced to increase linearly from 15‰ at 65 Ma to 23‰, its present day value (in that case, only the Li budget is solved, not C). Both simulations lead to similar trends, where Li_{soil} decrease as a function of time (see Figure 4). This strongly suggests the robustness of the observed decrease, and also confirms that the Li isotope composition of rivers plays only a minor role in the ocean isotopic variation. Overall, these results show that soil Li storage was high from 65 to 50 Myr, and then decreased continuously until its stabilization at about 20 Myrs ago (Figure 4).

In order to be more quantitative, check the consistency of these results and compare them to other proxies, we estimated the corresponding soil formation rates, assuming a Li concentration of 25ppm, which corresponds to an average soil Li concentration, including data shown in Table 1. This is a first approximation because secondary phase formation rate

(calculated from Li data) may not strictly correspond to soil formation rate. Also, the estimated average soil Li content may be associated with a large error, as there are currently only few data. It may also have varied as a function of time, although this is not supported by the relative narrow range of Li concentration of the most abundant clays. Nevertheless, this assumption allows us to assess if the order of magnitude for the fluxes extracted from our model makes sense. Also, a compilation of Li contents for the most abundant low-T continental clays show that the average Li value is not so different from one type of clay to another (Tardy et al., 1972; Table 1). During the Cenozoic, we thus estimate that soil formation rate ranged from $2.2.10^{19}$ kg/Ma to a present-day value of $1.3\ 10^{19}$ kg/Ma, i.e. $2.2.10^{10}$ t/yr to $1.3.10^{10}$ t/yr. For comparison, Syvitski et al. (2003) estimated a present-day global physical denudation rate of 2.10^{10} t/yr. The Syvitski denudation rate includes secondary phases and fresh minerals but the most important here is that both orders of magnitude are similar, and not totally at odd. Reconstitution of paleo-denudation rate during the Cenozoic are controversial (e.g. Willenbring & von Blanckenburg, 2010), but given the uncertainties typical of global scale estimations, it is worth noting that the calculated soil formation falls quite close (less than an order of magnitude difference) to the independent global denudation estimate, indicating that our calculations - based on C and Li cycles and published values for corresponding parameters - make sense. Considering the uncertainties on both estimations, a strict comparison between both numbers (physical and chemical erosion rates) in order to determine if the erosion regime has globally remained close to steady-state (where denudation rate and soil production rates are equal) during the Cenozoic does not appear to be relevant yet.

3.2 Assessing the role of climate

Except for the last few Ma, the paleo-reconstruction of soil formation rate during the Cenozoic is remarkably parallel to the $\delta^{18}O$ values measured in benthic foraminifera (Zachos et al., 2001, see figure 5B). This strongly suggests a major role of climate on soil development at the global scale. When the climate gets cooler, soil formation rates decrease. A potential increase of weathering rates due to orogenesis and mountain building during the Cenozoic is therefore not able to compensate the role of temperature. In the open debate concerning the controls of continental chemical erosion rates at global scale over the Cenozoic, Li isotopes yield good evidence of the predominance of climate over mechanical erosion. Specifically the fact that soil formation rates predicted by the model parallel the

global benthic oxygen isotope record shows that the impact of orogenesis is not strong enough to counter-balance the impact of temperature decrease.

More closely inspecting the comparison between soil formation rate, $\delta^{18}O$ and pCO_2 paleo-variations reveals four remarkable features:

1/ High soil formation rates during the Paleocene and Early Eocene, coincides with high pCO_2 estimations (Beerling and Royer, 2011) as well as low foraminifera $\delta^{18}O$ values. This strongly suggests that weathering rates were high because of climatic conditions favoring both dissolution of silicate rocks and formation of secondary minerals and laterites. In order to explain the high riverine $\delta^{7}Li$ values associated to low Li flux at this period of time (see Figure 3B), our budget equations require a massive transformation of fresh rocks into regolith. An important soil production also requires important weathering rates, consistent with high estimated atmospheric pCO_2 levels. This intense weathering leads to worldwide production of thick lateritic profiles, which is evidenced in many parts of the world (e.g. Beauvais and Chardon, 2013; Retallack, 2010; Tabor and Yapp, 2005; Robert and Kennett, 1992).

2/A sharp decrease of soil formation rate coeval with a sharp increase in foraminifera $\delta^{18}O$ during the Eocene until the beginning of the Oligocene. This co-variation suggests a predominant role of climate cooling on continental soil production. However, during this period of time, we cannot exclude a global thinning of soils by mountain building and orogenesis. Steeper slopes, higher relief, and increasing impact of landslide contribute significantly to reduce the world average soil thickness.

3/A stabilization of the weathering rates between 30 and 10Ma, which matches the plateaus exhibited by pCO_2 (not shown here, but see Beerling and Royer, 2011) and $\delta^{18}O$ proxies.

4/ A decoupling between soil formation rate, benthic foraminifera $\delta^{18}O$ and physical denudation rate during the Quaternary period. Indeed, both soil formation rates and pCO_2 estimates remain globally stable during this period. However, foraminifera $\delta^{18}O$ and denudation rates (e.g. Hay et al., 1988) show significant variations, consistent with the development of a cool climate and glaciations. Reconstructions of $^{10}Be/^{9}Be$ in the ocean also suggest a constancy of the continental weathering rates for the last 5-10 Ma and have questioned the relationship between physical and chemical erosion rates (Willenbring and von Blanckenburg, 2010). Our results suggest that the recent climatic variations were not strong enough to affect the Li cycle, as evidenced by constant foraminifera $\delta^{7}Li$ value during the last

5Ma. The other possibility is that the present-day residence time of Li in the ocean is underestimated and the chemical - and potentially physical - disturbances related to Quaternary glaciations did not have time yet to significant affect its oceanic budget.

3.3 Open questions

Our result for the Paleocene/Eocene boundary differs from previous modelings in two ways: first, the low ocean δ^7Li values at the P/E boundary may not necessarily require low riverine δ^7Li values, as previously considered in Wanner et al., (2014), in Misra and Froelich (2012) and in Li and West (2014). Secondly, at a period of time where weathering profiles are abundant and thick, Wanner et al. (2014) reactive transport model shows that low riverine δ^7Li such as observed at the Paleocene-Eocene boundary can be explained by predominant dissolution of previously formed secondary phases occurring in pre-formed thick regoliths (rich in kaolinite and goethite) (see section 2.5). The inverse relationship between regolith thickness and riverine δ^7Li arises from a longer residence time of water in contact with depleted secondary phases during periods characterized by weak tectonic activity and low physical erosion rates. In contrast, our model, which is based on budget equations only, implies that the formation of secondary phases from fresh bedrock produce an increase of river δ^7Li, because ^{6}Li is preferentially stored in regolith in formation.

Future studies should merge both methods such that transformation of the fresh bedrock into regolith and the building of thick weathering profiles can be accounted for, as well as the reactivity of the regolith itself.

The amount of published Li concentrations in various types of clay is still too limited to estimate precisely the Li mobility at the continental scale. At present, river particles carry more than 80% of the river total Li flux (calculation based on discharge and fluxes published by Gaillardet et al., 1999 and published average Li concentration for river water and suspended particles, Huh et al., 1998; 2001; Kisakurek et al., 2005; Millot et al., 2010; Dellinger et al., 2014). At 55Ma, the Li storage in soils is pretty close to 100% (following solution B). This corresponds precisely to the longest and one of the most intense weathering events of the Cenozoic in western Africa (Beauvais and Chardon, 2013), and probably elsewhere in the world (Rettalack, 2010). Conversely, case A predicts that only 20% of Li is retained during this event. Constraining more precisely the role of Li-rich kaolinite formation

485 in soils and laterites would certainly add precious information to the debate. A recent study of
486 Hawaiian basaltic soil chronosequence (Ryu et al., 2014) shows that Li is retained at 100% in
487 soil layers rich in kaolinite, which further supports their critical role, but more investigation at
488 larger scale is now required.
489
490 In our modeling , the hydrothermal carbon flux is assumed to be strictly compensated
491 by continental silicate weathering. The potential role of other sources/sinks of carbon has
492 been neglected at this stage, in particular the influence of metamorphism and of organic
493 matter burial. Indeed, disequilibria in the organic carbon subcycle may alter the
494 proportionality between the total CO_2 consumption by continental silicate weathering and the
495 CO_2 released hydrothermal activity. In the case of the strontium cycle for instance, it is well
496 known that such additional processes may produce non negligible fluctuations of the oceanic
497 isotopic composition (Goddéris and François, 1995). In the case of the Li cycle, these
498 processes are not expected to influence directly the Li fluxes and their isotope signatures.
499 However, change of carbon fluxes can potentially produce alteration of the Li isotopic
500 composition of the ocean. This is an important field for future investigations. The objective
501 here was to decipher the first order control factors on the time evolution of the Li cycle. The
502 calculated scenarii must be seen as a background history, neglecting at this stage processes
503 that could modulate the model output around the proposed long-term averaged evolution.
504
505 Although our model depends on the Li content of the continental silicate rock being
506 altered, there is no constraint on how these contents may fluctuate globally during the
507 Cenozoic. Determining how each rock type (basalt, granite, shales) contributes to the global
508 weathering flux, according to change in climate, vegetation and tectonic settings is beyond the
509 capability of our simple model. This aspect is currently explored with coupled 3D-
510 climate/biogeochemical models (Taylor et al., 2012; Lefebvre et al., 2013), showing for
511 example that the position of India relative to the tropical belt strongly controls the alteration
512 of the Deccan Traps lava flows. Exploring the impact of this on the lithium cycle is a task for
513 the future.
514
515
516
517
518

519 **4. Conclusion**

520

521 We provide a new approach for modeling the seawater δ^7Li record, preserved in marine
522 foraminifera and carbonate records (Misra and Froelich, 2012). The Li cycle includes several
523 fluxes of importance for the carbon cycle (and hence for the climatic evolution), including
524 continental weathering and hydrothermal water-rock interactions. For this reason, we have
525 combined the C and the Li cycles, so that our proposed reconstruction of the Cenozoic Li
526 cycle is compatible with the required stability of the exospheric carbon cycle at the geological
527 timescale (Walker et al., 1981). Results are consistent with the current knowledge of the
528 behavior of Li isotopes during continental weathering: 1/ in terms of isotope fractionation
529 during dissolution and clay formation 2/in term of present-day river flux and river δ^7Li.
530 We show that the paleovariation of the ocean δ^7Li through out the Cenozoic, can be explained
531 by significant Li stored on the continents during the Paleocene and Eocene, likely in
532 secondary phases which are Li-rich, such as phyllosilicates and oxides. Then this storage flux
533 globally decreases towards the present day, while the export to the ocean by weathering
534 increases. This storage follows indexes recording the climate evolution during the Cenozoic,
535 such as foraminifera $\delta^{18}O$ and pCO_2 reconstructions. More effort is now needed in order to
536 reduce the uncertainties associated with the Li cycle, and better deconvolve the role of erosion
537 from the one of climate during specific periods of the Cenozoic.
538

538 **References**

539

540

541 Beauvais, A., and D. Chardon Modes, tempo, and spatial variability of Cenozoic cratonic
542 denudation: The West African example, Geochem. Geophys. Geosyst., 14, 1590–1608,
543 doi:10.1002/ggge.20093, 2013
544 Beerling D. J., Royer D.R., Convergent Cenozoic CO_2 history, Nature Geoscience 4, 418-
545 420, doi:10.1038/ngeo1186, 2011
546 Berner, R.A., The Phanerozoic carbon cycle: CO_2 and O_2, Oxford University Press. pp160,
547 2004
548 Bouchez J., Von Blankenburg F. and Schuessler J. A., Modeling novel stable isotope ratios
549 in the weathering zone, Am. J. Science 313, 267–308, 2013, DOI 10.2475/04.2013.01, 2013
550 Burton K.W. & Vigier N. Lithium isotopes as tracers in marine and terrestrial
551 environments. Handbook of Environmental Isotope Geochemistry, 41-61, 2011
552 Chan, L.-H., W. P. Leeman, and T. Plank, Lithium isotopic composition of marine
553 sediments, Geochem. Geophys. Geosyst., 7, Q06005, doi:10.1029/2005GC001202, 2006
554 Chan L.-H., Edmond J.M.,Thompson G. and Gillis K., Lithium isotopic composition of
555 submarine basalts: implications for the lithium cycle to the ocean. Earth Planet. Sci. Lett. 108,
556 151–160, 1992
557 Chan L.-H., Edmond J. M. and Thompson G., A lithiumisotope study of hot springs and
558 metabasalts from mid ocean ridge hydrothermal systems. J. Geophys. Res. 98, 9653–9659,
559 1993
560 Chan L.-H., Gieskes J. M., You C-F and Edmond J. M., Lithium isotope geochemistry of
561 sediments and hydrothermal fluids of the Guaymas Basin, Gulf of California, ~, Geochim.
562 Cosmochim. Acta 58, 4443-4454, 1994
563 Dellinger M., Gaillardet J., Bouchez J., Calmels D., Galy V., Hilton R. G., Louvat P.,
564 France-Lanord C., Lithium isotopes in large rivers reveal the cannibalistic nature of modern
565 continental weathering and erosion, Earth Planet. Sci. Lett. 401, 359-372, 2014
566 Engebretson, D.C., Kelley, K.P., Cashman H.J., Richard M.A., 180 million years of
567 subduction, GSA Today 2, 93-100, 1992
568 Godderis Y., Francois L.M., The Cenozoic evolution of the strontium and carbon cycles:
569 relative importance of continental erosion and mantle exchanges, Chem. Geol. 126 169-190,
570 1995
571 Foustoukos, D.I., James, R.H., Berndt, M.E., Seyfried, W.E. Jr., Lithium isotopic

572 systematic of hydrothermal vent fluids at the Main Endeavour Field, Northern Juan de Fuca
573 Ridge. Chem. Geol. 212, 17-26, 2004
574 Hathorne, E. C., James, R. H.,. Temporal record of lithium in seawater: A tracer for silicate
575 weathering? Earth Planet. Sci. Lett. 246, 393–406, 2006
576 Hay, W. W., Sloan, J. L. I. & Wold, C. N. The mass/age distribution of sediments on the
577 ocean floor and the global rate of loss of sediment. J. Geophys. Res. 93, 14933–14940, 1988
578 Huh, Y., Chan, L.-H., Edmond, J. M, Lithium isotopes as a probe of weathering processes:
579 Orinoco River. Earth Planet. Sci. Lett. 194, 189–199 , 2001
580 Huh Y., Chan L-H, Zhang L., Edmond J. M., Lithium and its isotopes in major world
581 rivers: Implications for weathering and the oceanic budget, Geochim. Cosmochim. Acta 62,
582 2039–2051, 1998
583 Kisakurek, B., Widdowson, M., James, R. H., 2004. Behaviour of Li isotopes during
584 continental weathering: the Bidar laterite profile, India. Chem. Geol. 212, 27–44
585 Kisakürek, B., James, R.H., Harris, N.B.W., Li and δ^7Li in Himalayan rivers: Proxies for
586 silicate weathering? Earth Planet. Sci. Lett. 237, 387-401., 2005
587 Kump, L.R. and Arthur, M.A., Global chemical erosion during the Cenozoic:
588 Weatherability balances the budgets. In: Ruddiman, W., ed., Tectonics Uplift and Climate
589 Change, Plenum Press., N.Y., 399-426, 1997.
590 Lear, C. H., Elderfield, H. and Wilson, P. A., A Cenozoic seawater Sr/Ca record from
591 benthic foraminiferal calcite and its application in determining global weathering
592 fluxes. Earth and Planetary Science Letters 208(1-2), 69-84, 2003
593 Lefebvre V, Donnadieu Y, Goddéris Y, Fluteau F, Hubert-Théou L, Was the Antarctic
594 glaciation delayed by a high degassing rate during the early Cenozoic?, Earth Planet. Sci.
595 Lett. 371, 203-211, 2013
596 Lemarchand E., Chabaux F., Vigier N., Millot R., Pierret M-C, Lithium isotope
597 systematics in a forested granitic catchment (Strengbach, Vosges Mountains, France),
598 Geochim. Cosmochim. Acta 74, 4612–4628, 2010
599 Li G. and Elderfield H., Evolution of carbon cycle over the past 100 million years,
600 Geochim. Cosmochim. Acta 103, 11–25, 2013
601 Li G-J. and West A.J., Evolution of Cenozoic seawater lithium isotopes: coupling of global
602 denudation regime and shifting seawater sinks. Earth and Planetary Science Letters 401: 284-
603 293. doi: 10.1016/j.epsl.2014.06.011, 2014

Meshram R.R., Randive K.R., Geochemical study of laterites of the Jamnagar district, Gujarat, India: Implications on parent rock, mineralogy and tectonics, J. Asian Earth Sci. 42, 1271-1287, http://dx.doi.org/10.1016/j.jseaes.2011.07.014, 2011

Millot R, Vigier N, Gaillardet J, Behaviour of lithium and its isotopes during weathering in the Mackenzie Basin, Canada. Geochim. Cosmochim. Acta 74, 3897-3912, 2010

Misra, S. & Froelich, P. N., Lithium Isotope History of Cenozoic Seawater: Changes in Silicate Weathering and Reverse Weathering, Science 335, 818-823, 2012

Froelich F. and Misra S. Was the Late Paleocene-Early Eocene Hot Because Earth Was Flat? An Ocean Lithium Isotope View of Mountain Building, Continental Weathering, Carbon Dioxide, and Earth's Cenozoic Climate, Oceanography 27 (1), 36-49, 2014

Mottl, M.J., Seewald, J.S., Wheat, C.J., Tivey, M.K., Michael P.J., Proskurowski, G., McCollom, T.M., Reeves, E., Sharkey, J., You, C.F., Chan, L.H., Pichler T., Chemistry of hot springs along the Eastern Lau Spreading Center, Geochim. Cosmochim. Acta 75, 1013-1038, 2011.

Muller R.D., Sdrolias M., Gaina C., Roest W., Age, spreading rates, and spreading asymmetry of the world's ocean crust. Geochem. Geophys., Geosys., 9, doi: 10.1029/2007GC001743, 2008

Nahon D., Alterations dans la zone tropicale. Signification à travers les mécanismes anciens et/ou encore actuels. C.R. Geoscience, 335, 1109-1119, 2003

Retallack G.J.. Laterization and bauxitization events. Economic Geology, 105, 655-667, 2010

Retallack G.J., Cool-climate or warm-spike lateritic bauxites at high latitudes ? J. Geol., 116,558-570, 2014

Robert C., Kennett J.P., Paleocene and Eocene kaolinite distribution in the South Atlantic and Southern Ocean: Antarctic climatic and paleoceanographic implications. Mar. Geol., 103, 99-101, 1992

Rowley D.B., Rate of plate creation and destruction: 180 Ma to present. GSA Bull., 114, 927-933, 2002

Rudnick R. L., Tomascak P. B., Njoa H. B., Gardnerb L. R., Extreme lithium isotopic fractionation during continental weathering revealed in saprolites from South Carolina, Chem. Geol. 212, 45– 57, 2004

Ryu J-S, Vigier N, Lee S-W, Chadwick O, Variation of lithium isotope geochemistry during basalt weathering and secondary mineral transformations. Geochim. Cosmochim. Acta 145: 103-115, 2014

638 von Strandmann PAEP, Burton KW, James RH, van Calsteren P, Gislason SR, Assessing
639 the role of climate on uranium and lithium isotope behaviour in rivers draining a basaltic
640 terrain, Chem. Geol. 270, 227-239, 2010
641 Syvitski J.P.M., S.D. Peckham, Hilberman R., Mulder T., Predicting the terrestrial flux of
642 sediment to the global ocean: a planetary perspective, Sedimentary Geology 162 5 –24, 2003
643 Tabor N.J., Yapp C.J., Coexisting goethite and gibbsite from a high-paleolatitude (55°N)
644 late Paleocene laterite; concentration and 13C/12C ratios of occluded CO2 and associated
645 organic matter/ Geochim. Cosmochim. Acta, 69, 5495-5510, 2005
646 Taylor L.L., Banwart S.A., Valdes P.J., Leake J.R., Beerling D.J., Evaluating the effects of
647 terrestrial ecosystems, climate and carbon dioxide on weathering over geological time: a
648 global scale process-based approach. Phil. Trans. R. Soc. B, 367, 565-582, 2012
649 Tardy Y., Krempp G. et Trauth N, Le lithium dans les minéraux argileux des ciments et
650 des sols, Cosmochim. Cosmochim. Acta 36, 397-412, 1972.
651 Tavlan M., Thorne R. & Herrington R. J., Uplift and lateritization history of the Caldag
652 ophiolite in the context of Neo-Tethyan ophiolite obduction and uplift: implications for the
653 Cenozoic weathering history of western Anatolia, J. Geol. Soc. London 168, 927–940. 2011,
654 Teng F-Z, Rudnick R. L., McDonough W. F., Wu F.Y., Lithium isotopic systematics of A-
655 type granites and their mafic enclaves: Further constraints on the Li isotopic composition of
656 the continental crust, Chem. Geol. 262, 370–379, 2009
657 Tomascak, P. B., Developments in the understanding and application of lithium isotopes in
658 the Earth and Planetary Sciences. Rev. Mineral. Geochem. 55, 153–195, 2004
659 Vance, D. Teagle D.A.H. and Foster G.L. Variable Quaternary chemical weathering rates
660 and imbalances in marine geochemical budgets, Nature, 458, 493-496, 2009
661 Vigier, N., Gislason, S. R., Burton, K. W., Millot, R., Mokadem, F., The relationship
662 between riverine lithium isotope composition and silicate weathering rates in Iceland. Earth
663 Planet. Sci. Lett. 287, 434-441, 2009
664 Vigier N, Decarreau A, Millot R, Carignan J, Petit S, France-Lanord C, Quantifying Li
665 isotope fractionation during smectite formation and implications for the Li cycle. Geochim.
666 Cosmocim. Acta 72, 780-792, 2008
667 Wanner C., Sonnenthal E. L., Liu X.-M, Seawater δ^7Li: a direct proxy for global CO_2
668 consumption by continental silicate weathering? Chem. Geol. 381, 154-167, 2014
669 Wimpenny J., Gíslason S. R, James R. H, Gannoun A., Von Strandmann P., Burton K.W,
670 The behaviour of Li and Mg isotopes during primary phase dissolution and secondary mineral
671 formation in basalt, Geochim. Cosmochim. Acta 74 (18), 5259-5279, 2010

672 Walker J.C.G., Haysand P.B., and Kasting J.F. A negative feedback mechanism for the
673 long-term stabilization of Earth's surface temperature. J. Geophys. Res., 86(C10) : 9776–
674 9782, 1981.
675 Willenbring J. K. & von Blanckenburg F., Long-term stability of global erosion rates and
676 weathering during late-Cenozoic cooling, Nature 465, 211-214, 2010
677 Zachos, J. C., Shackleton, N. J., Revenaugh, J. S., Pälike, H., and Flower, B. P., Climate
678 response to orbital forcing across the Oligocene-Miocene boundary, Science 292, 274-
679 277, 2001
680 Zachos J.C., Dickens G.R., Zeebe R.E., An early Cenozoic perspective on greenhouse
681 warming and carbon-cycle dynamics, Nature, 451, 279-283, 2008
682
683

683

684 **Table 1:** Li concentrations measured in kaolinite (Tardy et al., 1972). These clays contain
685 0.2% MgO (Tardy et al., 1972). On average, the Li level for kaolinite is estimated to be 23
686 ppm. For comparison, average Li content for smectite is found to be 27 ppm (Tardy et al.,
687 1972) and 22 ppm for granites (Teng et al., 2009).

location	*Li (ppm*	*Reference*
Ivory Coast	30	Tardy et al. (1972)
	23	Tardy et al. (1972)
	53	Tardy et al. (1972)
	70	Tardy et al. (1972)
	22	Tardy et al. (1972)
	26	Tardy et al. (1972)
	4	Tardy et al. (1972)
	7	Tardy et al. (1972)
	7	Tardy et al. (1972)
	8	Tardy et al. (1972)
	32	Tardy et al. (1972)
	37	Tardy et al. (1972)
	5	Tardy et al. (1972)
	35	Tardy et al. (1972)
USA	20	Rudnick et al. 2004
Seine basin (France)	42	t.s.
Brasilian Amazon Basin	6.3	t.s
	5.3	t.s
	11.5	t.s
	11.8	t.s
Average Kaolinite	23	

688

Table 2: Parameters used the model. Δ_{oc} and Δ_{land} (Li isotope fractionation during secondary phase formation in the ocean and on land respectively) are chosen from within the published range, such that 1/ the seawater paleo-variation exactly match the 5Myr fit of the Misra and Froelich (2012) foraminifera data through the Ceonozoic (0-65Ma) (shown in figure 1) and 2/ at time t=0 (present day), both $F_{riv}(Li)$ and δ^7Li_{riv} values must be within the published range (see text for references).

	Published values	**Model values**
$\mathbf{F_{riv}(Li)}$	4-12.10^9 mol/yr	Free (see figures)
$\mathbf{F_{hyd}(Li)}$	2-145.10^9 mol/yr	5.10^9 mol/yr
$\mathbf{\delta^7Li_{hyd}}$	8.5±1‰	8
$\mathbf{\delta^7Li_{UCC}}$	1.7±2‰	1.7
$\mathbf{\delta^7Li_{riv}}$	23±2‰	Fixed at 23‰ / linear / free (see figures)
$\mathbf{\Delta_{oc}}$	10-25‰	14‰
$\mathbf{\Delta_{land}}$	10-25‰	23‰
$\mathbf{Li/C_{hyd} = 1/k_2}$		6.67.10^{-4}
$\mathbf{(Li/(Ca+Mg))_{UCC} = k_1}$		7.5.10^{-3}

Figure 1

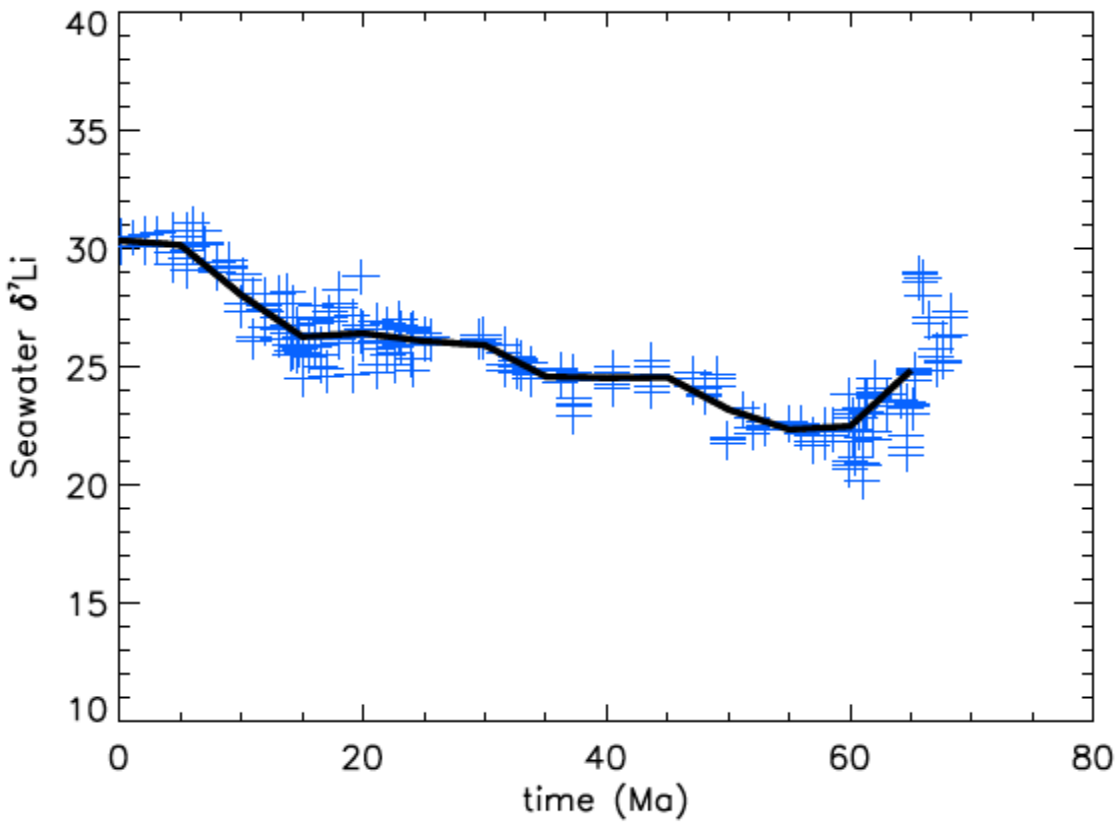

Figure 1: Seawater δ^7Li (in ‰) as a function of time (blue symbols), modified from Misra & Froelich (2012), assuming that marine foraminifera and carbonates reflect seawater composition. The black line shows a 5Myr moving average of the data. All model simulations performed in this study are forced to exactly fit this line.

Figure 2

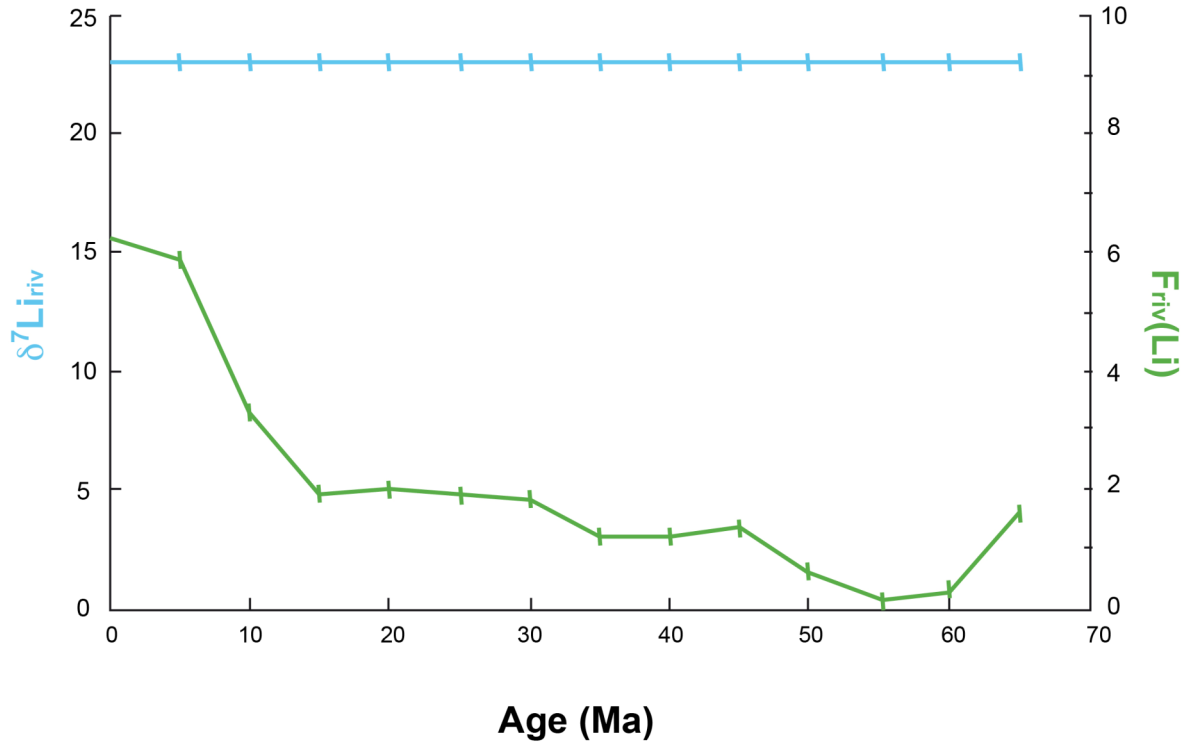

Figure 2: Simulation assuming constant δ^7Li_{riv} (in blue) as a function of time. As shown here, the seawater δ^7Li record presented in figure 1 can still be fitted if the flux of river Li (F_{riv} in 10^9 mol/yr, in green) increased significantly during the same period of time. This example demonstrates the lack of constraints on the steady-state model if only the equation for Li is considered. In addition this example shows that river δ^7Li can display temporal variations that are significantly different from the ocean δ^7Li record.

721 **Figure 3**

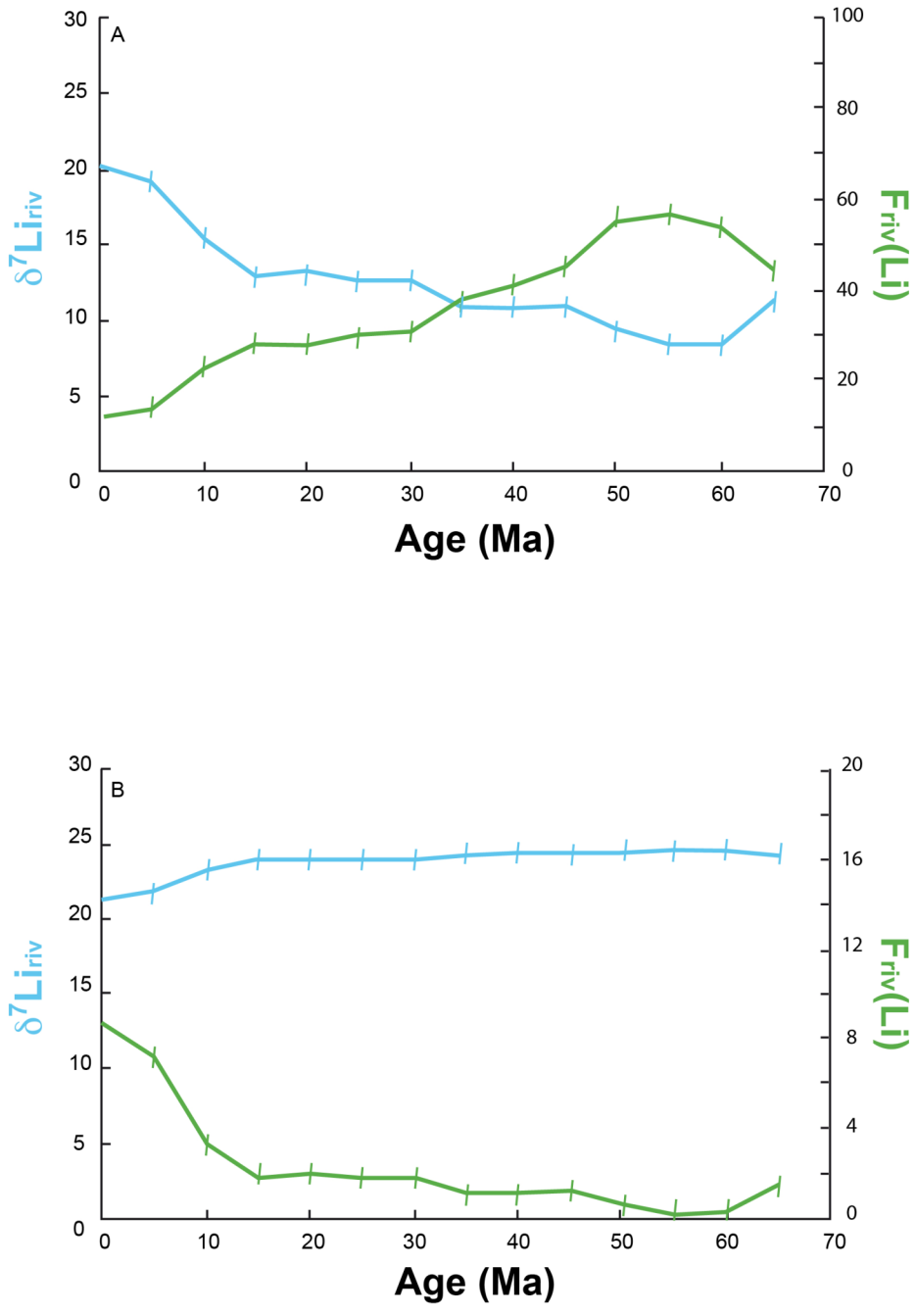

722

723 **Figure 3A&B:** The two solutions of the model described in the text that can both explain the
724 seawater record (see equations 3-12, and Table 2) F_{riv} is in 10^9 mol/yr (in green). **A/** this
725 solution is consistent with calculations performed by Misra & Froelich (2012) since low δ^7Li
726 values are found for 60Ma rivers and then increased as a function of time (in blue) **B/** a
727 second solution is also possible, using exactly the same set of parameters. In this case, river
728 δ^7Li has decreased as a function of time while the Li river flux has increased.

729

730

730 **Figure 4**

731

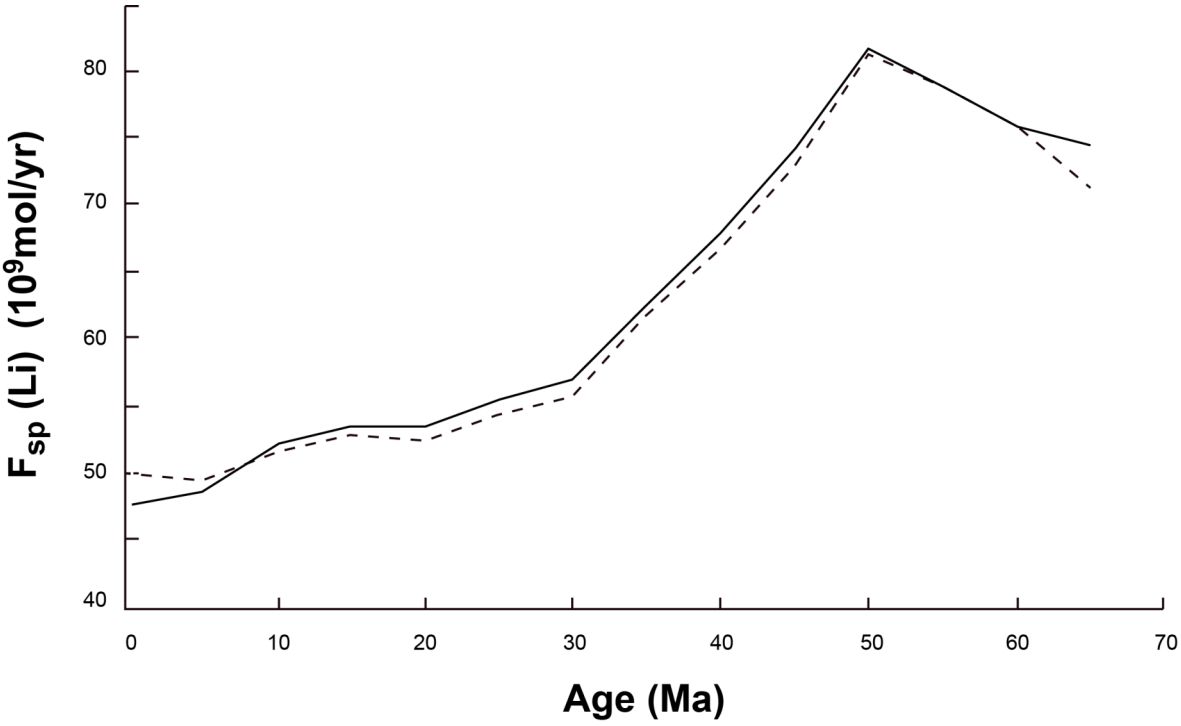

732

733

734

735

736 **Figure 4:** Flux of lithium incorporated into continental secondary phases as a function of time
737 (F_{sp}, see equation 6), following solution #2 of the modeling (shown in Figure 3B).
738 Comparison is made using a linear evolution for river δ^7Li as a function of time, from 15‰
739 (at 65Ma) to 23‰ (present-day) (dashed line).

740

741

742

742 **Figure 5**

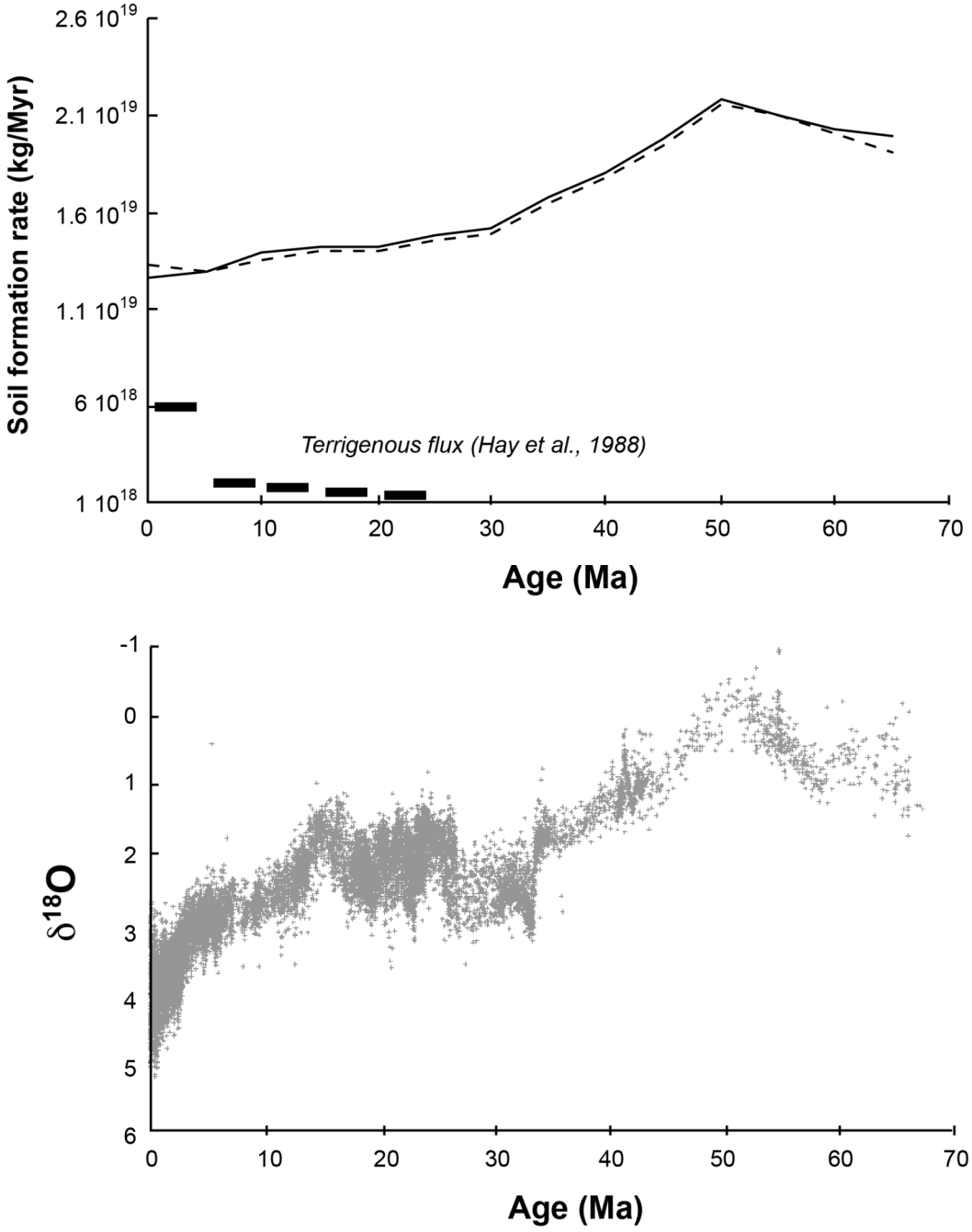

743

744 **Figure 5: A/** Evolution of soil formation rate as a function of time deduced from the
745 modeling of Li data and assuming that most secondary phases are formed in soils (see text for
746 more details). A published estimation of evolution of terrigeneous flux is shown for
747 comparison (same unit) **B/** Variation of $\delta^{18}O$ of benthic foraminifera as a function of time
748 (compilation from Zachos et al., 2001).

749